Bond formation at the Ni/ZrO_2 interface

J. I. Beltrán, S. Gallego, J. Cerdá, J. S. Moya, and M. C. Muñoz
Instituto de Ciencia de Materiales de Madrid, Consejo Superior de Investigaciones Científicas, Cantoblanco, 28049 Madrid, Spain
(Received 15 April 2003; published 7 August 2003)

We report on the formation of strong chemical bonds at the Ni(100)/cubic-ZrO_2(100) polar interfaces. *Ab initio* density functional theory calculations demonstrate that both Zr/Ni and O/Ni junctions are energetically stable, and predict that two different interactions determine the interface adhesion. Our results reveal that O-Ni ionic bonds are formed by Ni electron donation, while the Zr-Ni bonds show a mixed character with ionic and electron hybridization contributions.

DOI: 10.1103/PhysRevB.68.075401 PACS number(s): 73.20.−r, 68.35.Np, 73.90.+f

I. INTRODUCTION

Ni/ZrO_2 interfaces play a crucial role in a wide range of technological applications such as coating, heterogenous catalysis, fuel cells, microelectronic, optoelectronic or structural composites.[1] Most applications rely on the strength of the metal-ceramic bond. However, experimental studies suggest a weak interaction at the interface between Ni films grown on zirconia substrates.[2] Furthermore, Ni particles added to an Yttria-stabilized tetragonal zirconia (Y-TZP) matrix produce an embrittlement of the mechanical properties, which has been attributted to weak bonding between Ni and Y-TZP.[3] Consequently, the interface adhesion needs to be improved for an optimal performance of the Ni/ZrO_2 heterojunctions. The determination of the chemical basis of the metal-oxide interaction is a challenging task, due to its inherent complexity. Recent *ab initio* calculations allow to identify the metal adhesion mechanism in certain metal-ceramic interfaces,[4] suggesting that theoretical methods are useful tools to propose interfaces with good adherence. To our knowledge, the only first-principles study of the Ni/ZrO_2 system is the work of A. Christensen and E. A. Carter (CC).[5] As their main conclusion, CC predict that ZrO_2(111) adheres relatively strongly on a Ni(111) substrate at the monolayer level due to the formation of localized interface bonds, while for thicker ceramic films these bonds are weakened and the adhesion is dominated by the image charge interaction. Thus, this result suggests that if strong interface bonds are realizable for thick ceramic films, then the metal-ceramic adhesion energy could be sensibly increased. In this paper we report on the formation of such strong chemical bonds at the Ni(100)/ZrO_2(100) polar interfaces and show that two different interactions, Ni-Zr and Ni-O, may both provide the adhesion mechanism.

II. METHOD AND MODEL

All the results to be shown below were obtained after extensive calculations with the SIESTA (Ref. 6) density functional theory (DFT)-based *ab initio* code, employing the generalized gradient approximation[7] (GGA) for the exchange and correlation part. The main approximations in SIESTA are the replacement of the core electrons by norm conserving pseudopotentials[8] and the use of strictly localized numerical atomic orbitals (AO's) as the basis set. First, an exhaustive study was performed in order to optimize the basis set for the Zr, Ni, and O atoms, together with their respective pseudopotentials (including core corrections), until accurate results were obtained for different Ni and zirconia bulk phases. The spatial extension of the AO's, solely determined by the parameter $\Delta E(r_c)$ giving the energy required to confine the free atom AO within a radius r_c, was set to 100 meV after checking that this value yielded already well-converged results. In the case of Ni, we chose double-zeta (DZ) basis for the *s* and *d* AO's plus a single-zeta (SZ) *p* AO. Within DFT standards, accurate values for the lattice constants of fcc-Ni and bcc-Ni together with their respective magnetic moments were so obtained. The same type of basis set was used for Zr, whereas for O we employed DZ *s* and *p* AO's plus a SZ *d* AO. This choice correctly reproduces the energetic hierarchy among the three zirconia phases.[9] We recall that this is a quite demanding test due to the small energy differences between the phases ($\sim$100 meV/atom).

The nature of the bonds at the Ni/ZrO_2 interface, which is one of the central points of this paper, has been studied by means of charge density (CD) plots, together with energy resolved local density of states (LDOS) projected at specific atoms and crystal overlap population (COOP) analysis. The LDOS energy integration yields the Mulliken population for each projection, providing information on the electronic charge balance at each AO or atom (i.e., its ionic character). COOP's, on the other hand, determine the bonding (positive COOP values) or antibonding (negative values) character of the interaction between any two AO's or atoms, while their respective energy integrated quantites, denoted by bond order, may be viewed as the amount of charge shared in the bond. We recall that although these quantities are dependent on the choice of the AO basis set, they correctly give trends on the amount of charge transfer or the AO hybridization as long as the calculations are performed within a consistent scheme and are sufficiently accurate. Our calculations certainly meet both criteria.

The metal-ceramic interfaces are modeled following a supercell approach with periodic boundary conditions, stacking a Ni(001) two-dimensional (2D) slab on top of a cubic zirconia (c-ZrO_2) 2D slab also orientated along the (001) direction. Since $a_{c\text{-}ZrO_2} \approx \sqrt{2} a_{\text{fcc-Ni}}$, we aligned the Ni[100] and ZrO_2[110] crystallographic orientations, resulting in a small lattice mismatch at the interface (less than 2%). Based

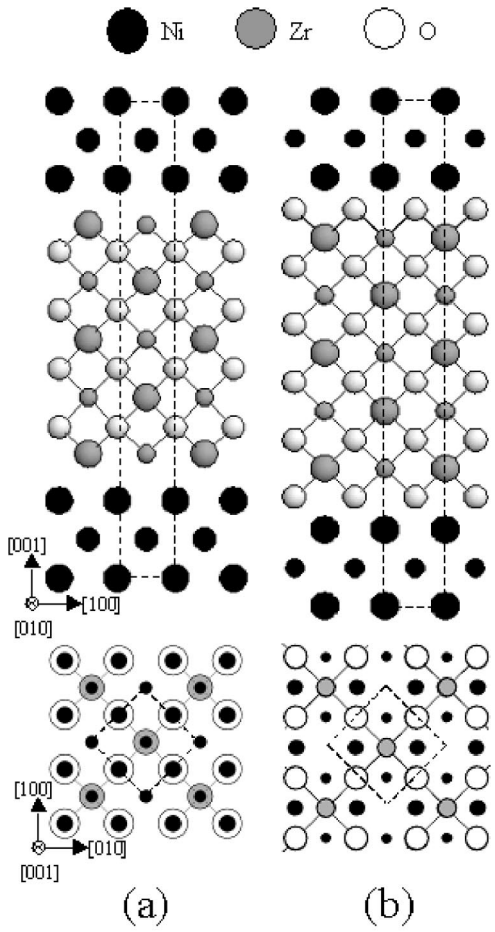

FIG. 1. (a) Lateral and top view of the c-ZrO_2/Ni(100) supercell used to simulate the Zr|Ni interface. (b) Same as (a) but for the O|Ni interface. Top views only include the atomic planes closest to the interface. Note that in (a), the Ni atoms are drawn even if they are located underneath another atom. In all views, the supercell unit cell is indicated by dashed lines, while the sizes of the atoms are set proportional to their depth.

on the fact that the oxide is more rigid than the metal, we modified slightly the Ni lattice in order to make it commensurate to that of the ZrO_2 slab with a $c(2\times2)$ coincident lattice, thus inducing a small in-plane tensile strain at the Ni slab. Along the (001) direction there are two different types of interfaces, Zr|Ni and O|Ni, depending on the termination of the polar ZrO_2 slab (either Zr or O atomic planes, respectively). We chose symmetric slabs for both Ni and ZrO_2 and no vacuum region, so that two equivalent interfaces are present per supercell (see Fig. 1). This choice ensures zero net dipole moments, and hence any unphysical dipole-dipole interactions between neighboring supercells is avoided. The Ni slab thickness was fixed to five layers, while for the Zr|Ni interface the ZrO_2 slab is consisted of nine layers [Fig. 1(a)] and for the O|Ni interface we included up to 11 layers [Fig. 1(b)]. We confirmed that for the above thicknesses, bulk-like behavior was already retrieved at the central layers of each slab.

DFT calculations were performed for different high-symmetry relative registries at both interfaces. In all cases, the atomic coordinates and the lattice vectors were fully relaxed until the forces on all atoms were less than 0.04 eV/Å, while the supercell Brillouin zone was sampled using a $(9\times9\times1)$ k supercell.

III. RESULTS AND DISCUSSION

The results of the study of the different registries for both the Zr|Ni and O|Ni interfaces lead to the most stable configurations depicted in Fig. 1. For the Zr|Ni case this corresponds to fourfold coordination of Zr to Ni atoms, the latter occupying equivalent positions to the nearest neighbor (NN) oxygen atoms in bulk ZrO_2 [Fig. 1(a)]. At the other interface, O|Ni, we find the Ni twofold coordinated to the oxygen atoms [Fig. 1(b)]. For both supercell geometries, lateral relaxations are negligible due to the high in-plane symmetries ($p4m$ and pmm) while, as expected from the Poisson effect, the in-plane tensile strain of the Ni slab is compensated by $\sim2\%$ compression of the vertical distance between Ni planes. For the O|Ni case, although the interplanar distances remain fairly constant throughout the ceramic slab, the $d_{\text{Zr-O}}$ closer to the interface slightly reduces.

Energetically, we find both interfaces favorable after comparing the total energies of each slab against the sum of the energies of the isolated (relaxed) ZrO_2 and Ni slabs. The resulting differences yield works of separation of $w_{\text{Zr|Ni}}=5014$ mJ/m^2 and $w_{\text{O|Ni}}=5743$ mJ/m^2, corresponding to rather strong metal-ceramic bonding. For instance, the reported work of separation for the Nb$|Al_2O_3$ interface,[4] which is known to be a system with an extremely good adherence, is $w_{\text{Nb}|Al_2O_3}=9800$ mJ/m^2. However, the above energy differences cannot be compared to the experimental work of separation, since many important contributions have not been considered: temperature, presence of crystal defects, vacancies and/or stabilizers, dissipative processes, large reconstructions that may appear at the ceramic polar surface, etc. Probably, a closely related but more meaningful quantity here is the bond strength, which we find to be 1.0 eV and 1.2 eV for the Zr—Ni and O—Ni bonds, respectively. These values are around five times larger than those obtained by CC for slabs of similar thickness.

The actual stability of each interface is given by the interface tension, $\sigma_{\text{ZrO}_2|\text{Ni}}$, defined as the Gibbs free energy normalized by the cross-sectional area A. Assuming that the interface is in thermodynamic equilibrium, neglecting the PV term and taking the zero temperature limit throughout, $\sigma_{\text{ZrO}_2|\text{Ni}}$ may be directly obtained from the total energy of the slab together with the number and the chemical potentials of each of the constituent atoms, N_i and μ_i, respectively:

$$\sigma_{\text{ZrO}_2|\text{Ni}}=(1/2A)(U_{\text{ZrO}_2|\text{Ni}}-N_{\text{Ni}}\mu_{\text{Ni}}-N_{\text{O}}\mu_{\text{O}}-N_{\text{Zr}}\mu_{Zr}).$$

Owing to the fact that our slabs are nonstoichiometric, we may express the last two terms as a function of the number of ZrO_2 units N_{ZrO_2} and its chemical potential μ_{ZrO_2} together with the excess/defect number of Zr atoms ΔN_{Zr} and the

deviation $\Delta\mu_{Zr}$ of the Zr chemical potential in the oxide μ_{Zr} from that in the pure hcp bulk phase μ_{Zr}^{hcp} (Ref. 10):

$$\sigma_{ZrO_2|Ni} = (1/2A)[U_{ZrO_2|Ni} - N_{Ni}\mu_{Ni} - N_{ZrO_2}\mu_{ZrO_2} - \Delta N_{Zr}(\Delta\mu_{Zr} + \mu_{Zr}^{hcp})].$$

For the Zr|Ni interface we have $N_{ZrO_2}=4$ and $\Delta N_{Zr}=1$, whereas for the O|Ni case $N_{ZrO_2}=6$ and $\Delta N_{Zr}=-1$. The chemical potentials μ_{Ni} and μ_{ZrO_2} have been computed according to $\mu_i = U_i^{N+1} - U_i^N$, where U_i^N is the total energy of a relaxed slab of material i containing N units, evaluated at a constant cross-section A (''stretched'' slab). We thus find negative values for $\sigma_{ZrO_2|Ni}$ at the Zr|Ni (O|Ni) interface for $\Delta\mu_{Zr} > -6$ eV ($\Delta\mu_{Zr} < -10$ eV). Notably, both values fall within the expected range of allowed $\Delta\mu_{Zr}$ values: $\Delta H_{ZrO_2} \leqslant \Delta\mu_{Zr} \leqslant 0$, with $\Delta H_{ZrO_2} = -11.37$ eV being the heat of formation per formula unit for zirconia.[11] The crossover between the two interfaces occurs at $\Delta\mu_{Zr} = -8$ eV, which corresponds to an interface tension of $\sigma_{ZrO_2|Ni} = 1.04$ J/m^2. This value indicates a better stability than for the ZrO_2/Ni(111) case studied in CC, where the interface tension was found to be $\sigma_{ZrO_2|Ni} = 1.80$ J/m^2. It is also worth mentioning that for $\Delta\mu_{Zr} > -8$ eV, the Zr|Ni interface is more stable than the O|Ni one, despite the fact that the work of separation is smaller for the former.

In the following, we characterize the nature of the bonds. Let us first concentrate on the Zr|Ni interface. The equilibrium Ni—Zr bond length is $d_{Ni—Zr} = 2.72$ Å, 0.12 Å smaller than the sum of their respective atomic radii, which is already an indication for the existence of a bonding between the two atoms. Figure 2(a) shows the LDOS projected at the interface and central layers. The LDOS in both central Ni and ZrO_2 planes are very close to those corresponding to the bulk crystals, apart from the location of the Fermi level in the oxide, which is shifted towards the conduction band minimum due to the finite size of the slab and the long screening length. In fact, interface effects are almost restricted to the atomic planes in contact, specially in the metal slab, where they are already screened at the second layer. Metal-induced gap states (MIG's) appear in the Zr LDOS with predominant s, xz, and yz character. On the Ni side there are also important changes in the occupied LDOS for both spin components. The characteristic three-peak fcc structure is lost and the d band is narrowed as a consequence of the reduction of nearest neighbors with respect to the bulk phase (10 vs 12 NN's). Interestingly, there is a reduction by a factor of 2 for the interface Ni magnetic moment (mm), $\sim 0.25\mu_B$, as opposed to the clean Ni(100) surface case, eventhough the reduction in the number of NN's is similar. The changes in the Ni LDOS shape affect most markedly AOs with z component. The Zr-Ni COOPs are also shown in the figure. They reveal a clear bonding character between Ni and Zr, which arises from s-d and d-d hybridizations. All the electrons in the occupied energy region attain positive values and hence, contribute to the bond. Notice, in particular, the strong peak for the MIGs states located at 1–2 eV below the Fermi level. For comparison, COOP's between two Ni adjacent layers located at the center of the slab are included. It is clear from this figure that more charge is shared in the Ni—Zr bond than in the Ni—Ni bond. Moreover, certain ionic character may be assigned to the Ni—Zr bond after inspection of the Mulliken charges quoted in Fig. 2. The interface Ni atoms, being more electronegative than Zr, gain 0.18e (that is, 0.09e per Zr—Ni bond), whereas Zr gains 0.44e with respect to the central layers, as a consequence of the replacement of four oxygens by two Ni atoms.

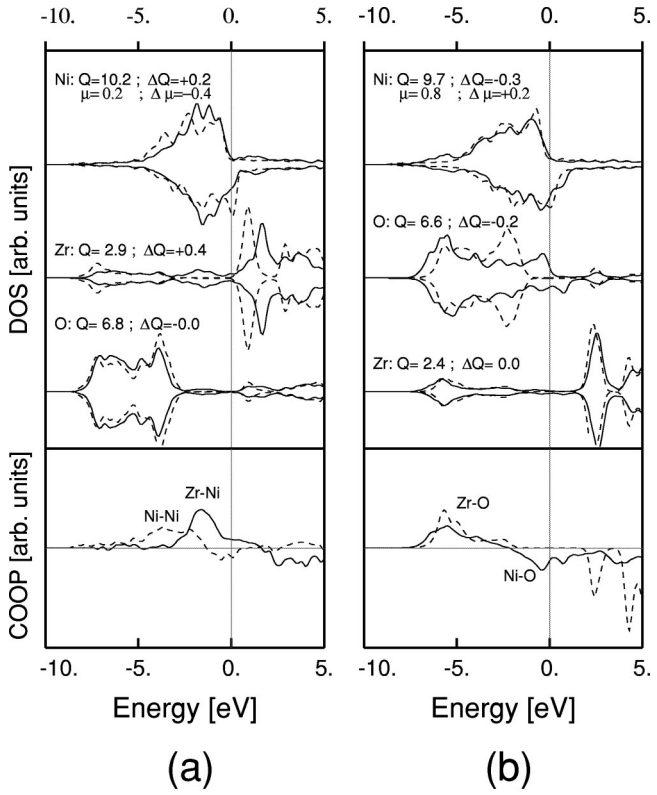

FIG. 2. Top graphs: Spin resolved LDOS for several atoms in the supercell corresponding to (a) the Zr|Ni interface and (b) the O|Ni interface. Solid curves correspond to the interface atoms in each supercell, while dashed curves correspond to the atoms at the center of each slab. Mulliken charges (Q) are given for each interface atom, while ΔQ refers to the charge difference between the interface atom and the corresponding atom at the center of the slab. The magnetic moment at the interface Ni atom and its difference with respect to the central Ni atom is also given in μ_B. Bottom graphs: COOPs between (a) the Zr—Ni interface atoms (solid line) and the Ni—Ni atoms (dashed line) and (b) the O-Ni interface atoms (solid line) and the Zr-O atoms at the center of the slab (dashed line).

Finally, we plot in Fig. 3(a) the CD differences (total CD minus a superposition of neutral atom CDs) for a cross section along the [110] and [001] directions including Ni, Zr, and O atoms. It is evident from the figure the mixed nature of the bonding. The Ni atoms develop a positive charge pointing to the Zr although fairly delocalized around the interstitial region, while the Zr experiences a loss of charge but in smaller amount than with respect to the back bonds with oxygen (notice the asymmetry of the negative CD isolines

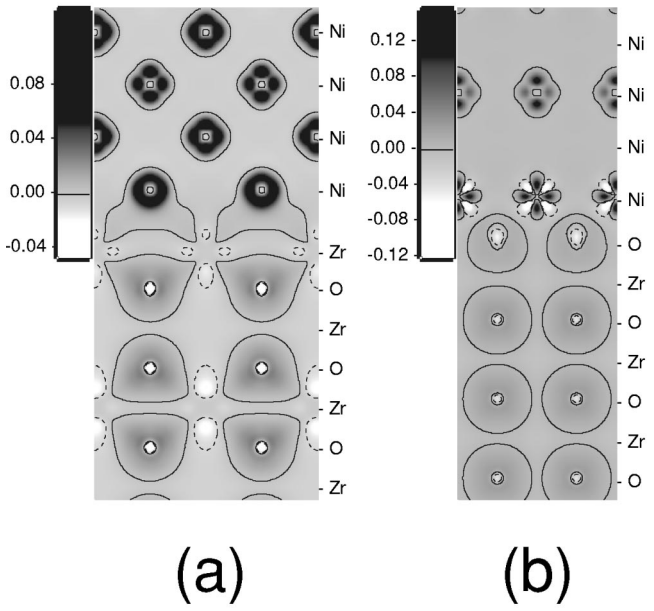

FIG. 3. Charge density (CD) difference (total CD minus superposition of atomic CD's) for (a) the Zr|Ni interface and (b) the O|Ni interface. As indicated in the adjacent legends, the linear gray scaling has been saturated so as to make features in the low-density regions clear. The solid contour line corresponds to zero CD difference, so that dark (light) regions give positive (negative) CD differences. A dashed isoline in the negative regions has been inserted in order to emphasize specific features in both 2D plots.

around the Zr in the figure). Moreover, both Ni spin components participate in the bond, since the spin density difference (majority spin CD difference minus minority CD difference) has a spherical shape slightly elongated in the in-plane lateral direction (not shown in the figure).

Next, we consider the O|Ni interface. We find an equilibrium Ni-O distance of $d_{\text{Ni-O}}=1.94$ Å, which is in the range of distances obtained at the ZrO_2/Ni(111) interface,[5] although in that case oxygen is one- or threefold coordinated. The Mulliken populations evidence that there is a net charge transfer from Ni to O. At the interface, Ni atoms have a charge reduction of $0.28e$—mainly from the sp and yz orbitals—which are gained by the O atoms. The oxygen has, in turn, $0.16e$ less than in the central layers, due to the smaller ionicity of the Ni—O bonds in comparison with the Zr—O bonds. In Fig. 2(b) the LDOS for the Ni and ZrO_2 interface planes are presented. As in the Zr|Ni case, induced interface effects show up as strong perturbations in the curves, but they are almost restricted to just one atomic plane in each slab. On the Ni layer the most important effect is the positive energy shift and broadening of the minority band, giving rise to an enhancement of the local mm by more than 30% ($\sim 0.8\mu_B$). Decomposition of the LDOS shows different shapes for the yz components and, to a smaller extent, for the xz, which stem from the broken $p4m$ 2D interface symmetry. Intrinsic interface states appear in the oxide energy gap, but also important changes within the band continua are seen for the oxygen. The position of the Fermi level at the MIG states corresponds to a metallic interface. All p-like oxygen LDOS are drastically altered and a non-negligible spin polarization is induced $\sim 0.2\mu_B$. However, Zr atoms are almost unaltered by the Ni presence. COOPs corresponding to the Ni|O interface atoms are represented in the lower graph of the figure. The Zr—O COOP for the bulk-like central layer is also included. Electrons in the energy region occupied by the oxide valence band have positive values, thus contributing to the Ni-O bond, while those at the band gap originating from the MIG's are negative. The compensation of the two regions leads to hardly any net charge sharing for this bond, indicating a pure ionic character.

Figure 3(b) shows the CD differences along the [010] and [001] directions containing the Ni and oxygen atoms (but not the Zr). The Ni atoms suffer strong modifications with respect to the metallic phase, presenting highly localized charge depletion regions (dashed lobes in the figure). On the contrary, the oxygen atoms experience minor modifications with respect to the bulk zirconia case: there is still a large and quite spherical charge pile up around the core apart from a negative nonspherical contribution inside the spheres. This picture clearly points to an ionic type O—Ni bonding. The CD difference maps are hardly spin dependent, except for the charge depletion at the O atom, which is dominated by the net spin density.

Our results show that Ni—ZrO_2 bonds are markedly stronger if the interface is along the $\langle 001\rangle$ direction than along the $\langle 111\rangle$. The larger work of separation and bond strength of the (100) interfaces can be correlated with the significantly smaller bond lengths: $d_{\text{Zr-Ni}}=2.72$ Å and $d_{\text{O-Ni}}=1.94$ Å, against $d_{\text{Zr-Ni}}=2.78$–2.88 Å and $d_{\text{O-Ni}}=2.02$–2.04 Å reported in CC. In order to rationalize these findings, it is convenient to highlight the differences between the interface modelization of CC and ours. In CC, the lattice mismatch is larger (5% vs 2%) while it is the ceramic film, the one holding all the in-plane strain. This strain is then released by a phase transition from cubic to pseudomonoclinic, so that intraceramic interactions seem to dominate over interface adhesion, leading to a weakening of the Ni-ZrO_2 bonds. On the contrary, in our calculation, the ZrO_2 slab has notably less degrees of freedom to relax, due to the almost negligible in-plane lattice mismatch, the absence of a ZrO_2 free surface close to the interface, and the lack of stress at the ceramic side. Hence, the ZrO_2 slab is largely inhibited to undergo strong restructuring, so that the main energy reduction arises from the Ni-ceramic bonding. Also, the interface bond density (number of interface bonds per unit area) is larger in our case: 0.3 bonds/Å^2 for both Zr|Ni and O|Ni versus 0.2 bonds/Å^2.

The above comparison suggests that the presence of strong Ni—ZrO_2 bonds should not be restricted to the $\langle 001\rangle$ epitaxial direction, but it could apply to any interface that presents good matching properties, namely, large bond densities, small lattice mismatch, and favorable initial atomic arrangements that avoid large relaxations within the ceramic film. Similar reasonings may be applied to other metal ceramic interfaces too. Further studies are required, however, in order to confirm if the current bonding mechanism persists in the presence of O vacancies and Y stabilizing defects.

IV. CONCLUSIONS

We have shown that the ideal Ni(001)/c-ZrO_2(001) interface is energetically stable. Works of separation corresponding to strong metal-ceramic bonds are obtained for both the Zr|Ni and the O|Ni interfaces. We predict that two different types of interactions can provide the interfacial bonding: Ni—Zr hybridization and ionic Ni-O bonding. The nature of the bonds and the corresponding charge distributions are described in detail. Our study provides potential useful information for the improvement of mechanical metal-ceramic adhesion, and we hope that it will motivate future experiments in this sense.

ACKNOWLEDGMENTS

This work was partially financed by the Spanish DGICyT under Contracts Nos. BFM2000/1330, MAT2001-1596, and MAT2000-1354. S.G. acknowledges financial support from the I3P Program of the C.S.I.C.

[1] C. Zhang and P.R. Norton, J. Nucl. Mater. **300**, 7 (2002); V.R. Choudhary, B.S. Uphade, and S.G. Pataskar, Appl. Catal., A **227**, 29 (2002); V. Fiorentini and G. Gulleri, Phys. Rev. Lett. **89**, 266101 (2002).

[2] D. Sotiropoulou and S. Ladas, Surf. Sci. **408**, 182 (1998); S. Harel, J.-M. Mariot, and C.F. Hague, *ibid.* **269–270**, 1167 (1992).

[3] S. López-Esteban, J.F. Bartolomé, J.S. Moya, and T. Tanimoto, J. Mater. Res. **17**, 1592 (2002).

[4] Y.F. Zhukovskii, E.A. Kotomin, P.W.M. Jacobs, and A.M. Stoneham, Phys. Rev. Lett. **84**, 1256 (2000); W. Zhang and J.R. Smith, *ibid.* **82**, 3105 (1999); **85**, 3225 (2000); Phys. Rev. B **61**, 16 883 (2000); I.G. Batirev, A. Alavi, M.W. Finnis, and T. Deutsch, Phys. Rev. Lett. **82**, 1510 (1999); C. Verdozzi, D.R. Jennison, P.A. Schultz, and M.P. Sears, *ibid.* **82**, 799 (1999); D.J. Siegel, L.G. Hector Jr., and J.B. Adams, Phys. Rev. B **65**, 085415 (2002); A. Bogicevic and D.R. Jennison, Phys. Rev. Lett. **82**, 4050 (1999); R. Schweinfest, S. Köstlmeier, F. Ernst, C. Elsässer, T. Wagner, and M.W. Finnis, Philos. Mag. A **81**, 927 (2001); S. Köstlermeier and C. Elsässer, J. Phys.: Condens. Matter **12**, 1209 (2000); E.A. Jarvis and E.A. Carter, Phys. Rev. B **66**, 100103 (2002).

[5] A. Christensen and E.A. Carter, J. Chem. Phys. **114**, 5816 (2001).

[6] D. Sánchez-Portal, P. Ordejón, E. Artacho, and J. M Soler, Int. J. Quantum Chem. **65**, 453 (1999).

[7] J.P. Perdew, J.A. Chevary, S.H. Vosko, K.A. Jackson, M.R. Pederson, D.J. Singh, and C. Fiolhais, Phys. Rev. B **46**, 6671 (1992).

[8] N. Troullier and J.L. Martins, Phys. Rev. B **43**, 1993 (1991).

[9] G. Jomard, T. Petit, A. Pasturel, L. Magaud, G. Kresse, and J. Hafner, Phys. Rev. B **59**, 4044 (1999).

[10] I.G. Batirev, A. Alavi, and M.W. Finnis, Phys. Rev. B **62**, 4698 (2000); W. Zhang and J.R. Smith, *ibid.* **61**, 16 883 (2000); W. Zhang, J.R. Smith, and A.G. Evans, Acta Mater. **50**, 3803 (2002); X.-G. Wang, A. Chaka, and M. Scheffler, Phys. Rev. Lett. **84**, 3650 (2000).

[11] H.Y. Affeefy, J.F. Liebman, and S.E. Stein, *Neutral Thermochemical Data*, in *NIST Chemistry WebBook, NIST Standard Reference Database Number 69*, edited by W.G. Mallard and P.J. Linstrom (National Institute of Standards and Technology, Gaithersburg, MD), http://webbook.nist.gov